

Improved Detection and Extraction of Human Life Sign Hidden Behind the Brick Wall Using Stepped-Frequency Continuous Wave Radar

Abhay N Gaikwad

Department of Electronics and Telecommunicatio, Babasaheb Naik College of Engg. Pusad, Maharashtra,

Abstract : *In this paper, a technique for significant improvement in detection of breathing signal of a human being hidden behind brick-wall has been developed. Presence of clutter due to strong reflections is a problem in detection of breathing signal. The reflected signal from the target might be completely overridden by clutter and thus it requires to be reduced. Singular value decomposition (SVD) is proposed to reduce clutter and strengthen the target signal. Experimental setup based on Step Frequency Continuous wave (SFCW) radar system in ultra wideband (UWB) frequency range has been used. It is observed from the experimental results that after application of clutter reduction technique, there is a significant improvement in the target signal strength and also in detection and extraction of the breathing signal.*

IndexTerms - *Fast Fourier Transform (FFT), Life sign, Step Frequency Continuous Wave (SFCW) radar, Singular Value Decomposition (SVD).*

I. INTRODUCTION

Human beings have always been interested to find out the unknown from the very beginning of the history of a mankind. A human eye helps to investigate the environment by the reflected light. However, wavelengths of visible light allow a transparent view through only non opaque materials such as glass and not through the opaque materials. On the other hand, electromagnetic waves with frequencies in the range of microwaves are able to penetrate through almost all types of materials except metal. RADAR sensing with electromagnetic waves is an emerging technology, allowing us to see through visually opaque materials [1].

Non-contact detection and extraction of human life sign is a cardinal issue in many applications such as homeland and military security involving localization, detection and monitoring human activities hind side of the brick-walls in connection with law enforcement and surveillance, localization and rescue of living survivors buried under rubble and debris of building in post earth-quake scenario, health care etc [2]. Due to the mentioned significance of this topic, there has been growing interest of researchers in this field. In recent years this has resulted in large improvement in the technology entailed. Radar signals reflected from the living target carry the information about their vital signs [3].

In this paper, work is carried out to address one of the applications of radar sensing, i.e., detection of life sign, when the person is standing behind the brick-wall and is still and cannot make movement. It represents a simplified case compared to the situations in earthquakes and collapsed buildings where the human being is trapped under rubble. Here instead of rubble, brick-wall is considered as a barrier between radar and human being. The life signs of human being which are normally used for the detection are breathing/respiration rate and heart rate. In this paper, the detection of breathing signal is carried out which is enough to know the presence of life in human being.

In the past decade, the researchers were mainly working on microwave radar based sensor system for life sign detection. Ultrasound, millimeter wave radiometry, infrared, and X-rays can be used for seeing through visually opaque material but Radar sensor is the most suitable due to various reasons such as; ultrasound technique can be used to detect and find target behind a metallic or non-metallic brick-wall but cannot be used when high resolution is required. Millimeter wave radiometer uses energies radiated by bodies of targets for the detection and is limited to work only up to a very short distance. Infrared can be used to image the target through opaque material only for very short distance as attenuation through a brick-wall is very high. X-ray based sensors provide good resolution quality but are limited due to their high cost and lack of medical safety [1], [4].

Researchers are using either continuous wave (CW) or pulse based radar technique. CW radar are of two types, first frequency modulated continuous wave (FMCW) radar and second step frequency continuous wave (SFCW) radar. FMCW based radar system depends on the difference in received and reference frequency. SFCW radar system depends on the phase difference between receiver and reference signal. Pulse based radars like ultra wide band (UWB) pulse radar and UWB noise radar have also been used in recent times by different research groups [5]. Using CW radar, the detection of life sign has been reported without localization [6]. It has been observed that in FMCW radar system, resolution is lower due to which it cannot easily separate multipath signals or strong reflections from static barrier such as a brick-wall. Compared to this, pulsed radar can detect and locate multiple vital signs and have better resolution because of large bandwidth under low SNR [7, 8]. Impulse radar has fast data acquisition though dynamic range is not as good as SFCW radar. Moreover latter has good resolution of range and power [2]. These key advantages and features associated with SFCW radar led the researchers to utilize SFCW radar for life sign detection behind the brick-wall. Hence, it was decided to use SFCW based radar system for this work.

In radar, an electromagnetic wave is transmitted by the transmitting antenna; the signal penetrates through the brick-wall and is reflected by the human subject, again penetrates through the brick-wall, and is received back by the receiving antenna. The reflected signal is received and processed by the radar. In this radar technology, because of heartbeat and respiration of human being, modulation of incident radar signals occurs, which are demodulated to extract vital sign [3]. The signal processing is used to find out living targets if any, present behind the brick-wall. The first objective is to detect target and extract the location of target behind the brick-wall or opaque material. The second objective is about extracting life sign. Presence of clutter is a problem in the detection. The reflected signal from the human being (target) might be completely overridden by clutter and thus necessitates processing to improve target signal strength.

Earlier researchers have used different techniques to improve signal strength. Range gating, background subtraction, notch filtering and moving average reductions are some of them [9]-[13]. In background subtraction method, scans of received signal without target behind brick-wall are subtracted from scan with target behind the brick-wall to mitigate the effect of brick-wall. But it is impossible in practical situation to

get data without presence of target [13]. Clutter suppression has been achieved by simple method of subtracting each of the range profile from previous to eliminate components that have not changed [14]. A simple low pass FIR filter called Moving Average Filter has been proposed [15],[16], which is used to smooth the data by taking an average of samples of input data to produce single output thus eliminating noise. Most of the clutter is associated with zero frequency or DC term and its multiple integers of pulse repetition frequency thus suppresses clutter by offering deep stop band to these frequencies have been reported by using MTI filtering [17] where mean of all range profile is subtracted from current one to get moving part. In [18], Spatial filters, which notches out the zero spatial frequency components has been effectively used for removal of clutter signal from brick-wall. Linear Trend Subtraction (LTS) method has been demonstrated to suppress the pulse amplitude variation in [19].

To remove brick-wall clutter, researchers working in through the brick-wall radar imaging area have used SVD. In synthetic aperture radar (SAR) technique, first, data is collected at different positions in the scanning direction and then SVD is applied. In this paper, SVD is applied by collecting several data at same antenna positions. In SVD, dominant *Eigen* image of target is considered though residue is present in many *Eigen* images [20]. Target signal strength can be improved by removing brick-wall reflections. In [21], SVD has been used after taking the Fast Fourier Transform (FFT) of correlated signal. But we propose used of SVD for clutter reduction before applying FFT. Other effects due to presence of brick-wall are refraction, attenuation and change in velocity of the signal which poses challenges for the detection and localization.

Another problem is to detect the breath or respiration frequency and heart beat frequency under severe clutter contamination. Researchers have carried out work on detecting and extracting life sign of human being using different signal processing techniques which is briefly given here. Motion of human being has been detected by using change detection algorithm [13]. Life detection algorithm is carried out by picking up time record of the periodic variation along the recording time at a given propagation time in SFCW radar [2]. In [22], researchers have proposed Generalized incoherence factor (GICF) and Filter bank based generalized coherence factor (FBGCF) methods to detect and estimate respiration. In [23], filters are used for extraction of life sign of targets. The FFT algorithm gives data about human micro and macro movement's frequency and amplitude. Extraction of vital sign has been demonstrated with FFT algorithm in our earlier work where plywood was used instead of brick-wall [24]. In present paper, plywood wall is replaced by brick-wall to see the effect on the detection of breathing signal. In [2] respiration frequency has been detected for different positions of human target behind brick-wall but there is further scope for improvement in signal processing. Life sign detection behind the corner of brick-wall considering diffraction of signals at corner with SFCW radar is demonstrated in [25]. Short time Fourier transform (STFT) signal processing is used which maps a signal into a function of time and frequency. Breathing signal has been detected with STFT [6]. However the results are from ideal conditions and multipath data has not been addressed. Experiments have been performed on Gypsum wall, brick-wall, wooden door and concrete wall with UWB pulse radar with center frequency of 4.3 GHz [26]. Heart beat frequency and breathing frequency has been detected in all cases except concrete wall and gypsum wall when SVD and STFT were used. Mono static mode limits the use of spatial filtering to reduce clutter and also STFT has got fixed resolution.

Authors have described a method based on MUSIC algorithm applied to echo data collected from CW radar with 10 GHz centre frequency to detect breathing signal [27]. The algorithm used in [27] has been further modified by authors in [28] where SNR is improved compared to previous method. This algorithm detects only main harmonic components of spectral noise since it can add or delete close harmonics which are not placed in pre-known position. Thus this can be used to detect particular harmonic component with presumed frequency. A multiple higher order cumulant based life sign detection method is presented in [29] and have improved the detection further using constant false alarm rate (CFAR) and clustering method in [30], but have failed to address the effect of presence of strong clutter.

In a nutshell, considerable amount of attention and research work is required for dealing with different issues related to life sign detection. This motivated us to develop signal processing techniques to improve the detection, localization and extraction of life sign of the living targets, hiding behind brick-wall.

The methodology adopted is described in Section II, which includes measurement setup, data collection details and the theory of signal processing applied on data. Analyses of experimental data are discussed in result Section III. Finally conclusions are given in Section IV.

II. METHODOLOGY

The methodology is to initially develop an experimental setup based on SFCW radar system, then collection of data and finally to process it to extract the breathing frequency. Following subsections describe the work undertaken. Major processing steps consist of pre-processing, detection and extraction of information like breathing/respiration frequency.

A. Experimental Setup

To extract breathing signal of human target, measurements using an experimental setup as shown in Fig.1 is carried out in corridor of college building. The experimental setup consists of antennas, Vector Network analyzer (VNA), Laptop, cables to connect them and human being as a target standing behind brick-wall. The VNA based SFCW radar system is placed on the front side of brick-wall. The radar specifications used for the experiments are given in Table 1. The two antennas have a gap of 0.30 m between them. Tripod is used to adjust the height of antennas to align it with a human chest. The orientation of the antenna for data collection is vertical polarization. The dimension for brick-wall is 5 × 6 feet with thickness of 10 cm. Data are collected with presence and absence of human target. The total distance between the human target and radar is varied.

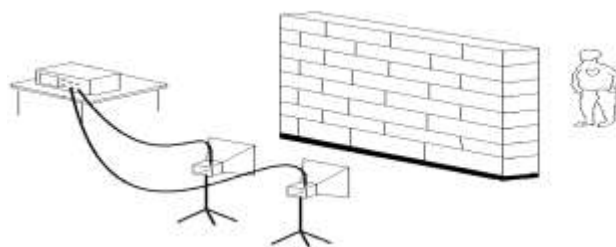


Fig.1. Experimental Setup

B. Data Collection

Experiment was carried out in three stages to collect three sets of data. In the first data set, human being (target) is absent, whereas in second and third data set the target is present. Measurements were done on a 26 year old male test subject. The distance between brick-wall and target (human being) is varied whereas the distance between antennas and brick-wall is kept constant in all measurements. In the second set, antenna to human target distance is 1m whereas in third set, it is 1.5m. Two port standard calibrations is done for measurement of transmission parameter S_{21} in UWB frequency range i.e., 1 GHz to 3 GHz. Reflections from closely spaced targets in range can be achieved if bandwidth (BW) is 2 GHz which gives 7.5 cm as range resolution. The scan or trace is repeated 1024 times to observe the changes in returned signal over time. The acquired data is saved for every measurement. Every measurement is organized as a matrix as shown in Table 2, in which each row represents the number of frequency points ($N=201$) and column represents number of traces ($M=1024$). For each trace, reflected signal (S_{NM}) where $N=1$ to 201 and $M=1$ to 1024 in complex data form in frequency domain is stored as shown in Table 2.

Table 1. Radar specifications

Parameters	Values
Frequency Range	1 to 3 GHz
Transmitted Power	10 dBm
Number of Frequency points	201
Number of Traces	1024
Antenna Type	Horn
Gain of Antennas	20 dB
3 dB Beam width of Antennas	49.68(H-plane), 59.36 (E-plane)

Table 2. Matrix representing organization of data collected

Trace No. / Frequency. No.	1	2	3	4	...	M
F ₀	S ₁₁	S ₁₂	S ₁₃	S ₁₄	...	S _{1M}
F _{0+Δf}	S ₂₁	S ₂₂	S ₂₃	S ₂₄	...	S _{2M}
...
F _{0+(N-1)Δf}	S _{N1}	S _{N2}	S _{N3}	S _{N4}	...	S _{NM}

C. Signal Processing Algorithm

Signal processing is applied to obtain the spectral content of the reflected signal from the human being due to chest movement caused by respiration and heart beat. Flowchart in Fig. 2 described the steps in signal processing algorithm.

Step 1. Read Trace data in Frequency domain

The SFCW radar source transmits continuously equal and linear spaced frequency with start frequency as F_0 and stopped at $F_0+(N-1)\Delta f$ as shown in Table 2. SFCW radar received the data in frequency domain, and stored as shown in Table 2. To read the first trace, column 1 data is picked up and filtered by Hamming window [17]. Side lobes can be reduced by applying Hamming window which in turn increases dynamic range.

Step 2. Convert Frequency domain to Time domain

After windowing, time domain data is obtained by using the Inverse Fast Fourier Transform (IFFT). The signal received $S(f_n)$, after IFFT is given by [31],

$$s(t) = \sum_{n=1}^N S(f_n) \exp(j2\pi f_n t) \quad (1)$$

where N is maximum number of frequency points and t varies with step interval of $1/BW$.

Step 3. Convert Time to spatial domain

Range profile is constructed to obtain the location of target. Range profile is obtained by converting time domain signal into spatial domain. Range profile which is one dimensional information is represent

$$S(z) = \sum_{n=1}^N S(f_n) \exp(j2\pi f_n(2z/c)) \quad 0 < z < z_{\max} \quad (2)$$

where z is down range distance given as

$$z = (c \times t) / 2 \quad (3)$$

and c is velocity of light. The maximum distance Z_{\max} and range resolution ΔR are determined by following formulas:

$$Z_{\max} = c(N-1)/2BW \quad (4) \text{ and}$$

$$\Delta R = \frac{c}{2N\Delta f} \quad (5)$$

where Δf is step size.

These are the basic steps that are implemented before processing the signal for further analysis to retrieve information which are described in next section.

Step 4. Stacking all traces to form data matrix

A single range profile is insufficient to provide information about presence of life sign of human target. More number of range profiles must be observed. Data matrix is formed by stacking all the range profiles.

Step 5. Apply Clutter reduction technique

Due to reflection from brick-wall, the major problem is loss of energy. Due to air brick-wall interface, strong reflection occurs. Thus very small amount of energy reaches to the human target after passing through brick-wall. Again at target, due to dielectric contrast between air and human being, reflections take place. This reflected signal reaches back to radar side. Thus strength of signal is further weakened. The reflected signals which reach to radar other than human target are called as clutter. Thus for human target detection, clutter reduction cannot be ignored. Clutter reduction is carried out using the SVD technique which separates target from clutter data.

Consider data matrix with dimensions $N \times M$; and $(i = 1, 2, \dots, N; j = 1, 2, \dots, M)$, where the i represent distance (down range) and j represents number of traces. Representation of SVD is given as:

$$X = USV^T \quad (6)$$

where T denotes Hermitian transpose, unitary matrices U and V are $(N \times N)$ and $(M \times M)$ sizes respectively, and S is $N \times N$ diagonal matrix. Singular values are arranged in decreasing order i.e., $\sigma_1 \geq \sigma_2 \geq \dots \geq \sigma_i \geq 0$. The decomposition of X matrix is given as:

$$X = \sum_{i=1}^N \sigma_i u_i v_i^T \quad (7)$$

or

$$X = X_1 + X_2 + \dots + X_N \quad (8)$$

where X_i are called as i^{th} Eigen image of X . There is a need of to identify Eigen image that represents target response. After comparing results obtained using SVD for absence and presence of the target, it is concluded that the second column of U (u_2) i.e., second singular component represent target. The response of target (T_1) is given by:

$$T_1 = X_2 = \sigma_2 \times u_2 \times v_2^T \quad (9)$$

T_1 represents the Eigen image of target response only. Since the brick-wall reflections are stronger than target reflections, the dominant first singular value represents brick-wall subspace. Also while taking measurement it is ensured that the antenna is perpendicular to the brick-wall surface i.e., antenna is not tilted at any angle with respect to brick-wall surface and also the brick-wall thickness remains same for all the measurements, the clutter subspace does not span to multidimensional subspace [20]. However, the target subspaces do not remain single subspace and may span to multidimensional subspace as there is variation of amplitude values at target location. So instead of considering only second singular components as used in equation (9), all the singular components related to target should be used. Since all N indices do not contribute to target subspace, there is need to determine which singular components relates to target subspace. The distance from range profiles are observed to find out the corresponding singular components. The target subspace is obtained using multiple singular components as shown in (10);

$$T_2 = \sum_{i \in \tau} \sigma_i \times u_i \times v_i^T \quad (10)$$

where τ is

a set of all indices for target singular vectors.

Step 6. Find location of target using standard deviation (SD)

Signal processing should be carried out in such way so that radar operator can understand the presence or absence of human target. Using SD method, amplitude at each distance in every range profile is observed. If life sign is present, then at target location there will be amplitude variations in all 1024 traces due to chest movement caused by respiration and heart beat. To observe whether there is amplitude variation or not, standard deviation (SD) is calculated using (11).

$$SD_d = \sqrt{\frac{1}{M} \sum_{m=0}^{M-1} (x_i - \mu)^2} \quad (11)$$

where d is distance and M is number of traces.

The location at which maximum value of SD is obtained is considered as human target location.

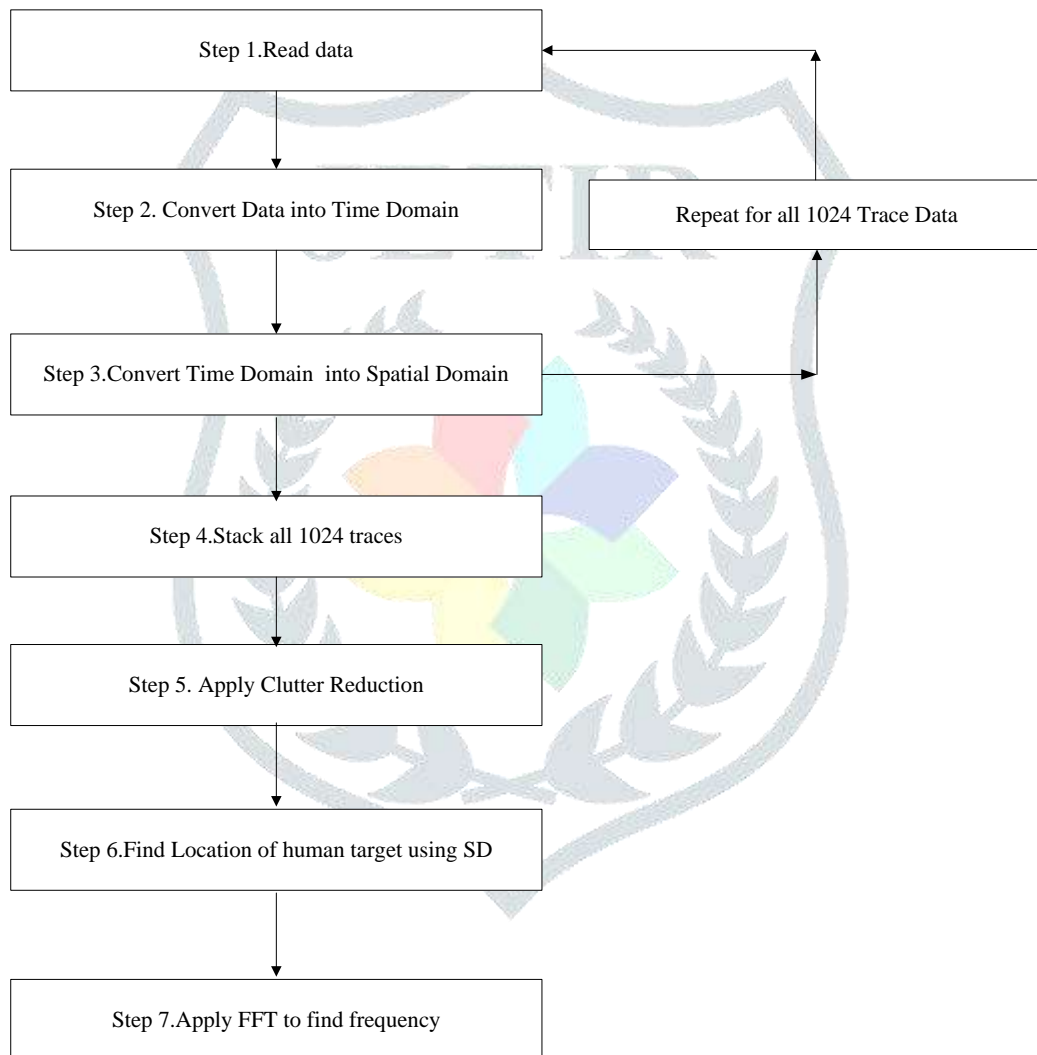


Fig.2. Flow-chart for processing steps

Step 7. Extraction of breathing frequency using the Fast Fourier Transform Method

Once the location is obtained, following steps are applied before the Fast Fourier transform (FFT) method is used. Extract amplitude values from the obtained location. Since there is fluctuation, instead of extracting amplitude value from one location, amplitude of succeeding and preceding locations are also picked up and their average is taken. As there are 1024 traces, total number of average amplitude values will be 1024. Normalize the amplitude values between ± 1 . Now apply FFT algorithm on the normalized extracted signal to convert into frequency domain signal. The breathing frequency for normal human being corresponds to frequencies 0.2 to 0.5 Hz while heart rate corresponds to 0.8 to 1.5 Hz. Since we are interested in frequencies in the range of 0.2 to 1.5 Hz, a second order band pass filter using Butterworth is applied.

III. Result and Discussion

The aim is to improve the detection of life sign by reducing stationary clutter. The three sets of data collected experimentally are processed. In the first set the target is absent, in second set the distance between radar and standing human being is set as 1m and in third set it is 1.5m. The processing is done according to the flowchart described in Fig. 2. Results for these sets of data is discussed below.

A. Absence of human target

First set of data is considered for processing which is taken without human target. All the range profiles are overlapped on each other to observe amplitude variations and are shown in Fig. 3. Distance against magnitude is plotted in it. Though maximum distance obtained using (4) is 15 m, it is taken upto 5 m only. In absence of target only three peaks as shown in Fig. 3 are observed. First peak represents weak isolation between antennas. Second and third peak represents reflections from front side and rear side of brick-wall. Since the radar is used in UWB range, it resolve front and rear side of brick-wall as thickness of brick-wall is greater than range resolution. As human target is absent, no amplitude variation is observed. The remaining small peaks observed thereafter are due to the multipath reflections.

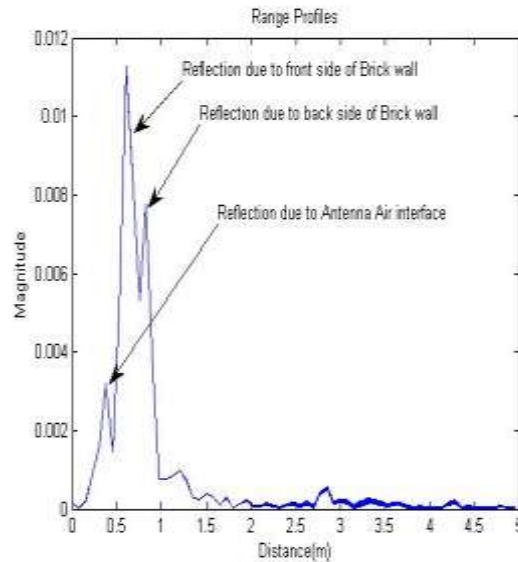
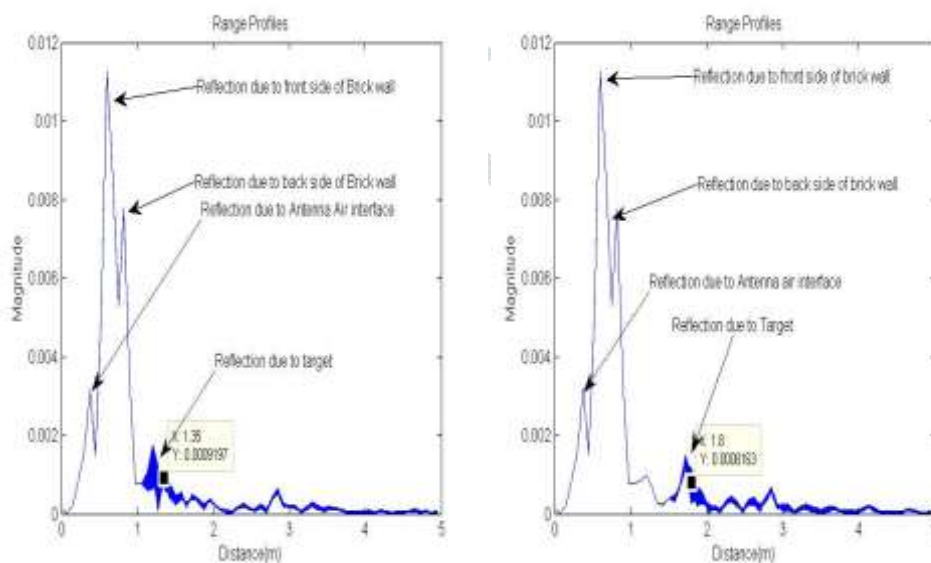


Fig. 3. Range profiles in absence of human target

B. Presence of human target

Detection of human target can be obtained from more number of traces by observing amplitude variations at target location due to breathing/respiration. Figure 4 (a) and (b) shows all the range profiles stacked one over other to observe amplitude variations for second and third set of data. Additional peak compared to Fig. 3, is observed due to presence of human target which is shown in Fig.4 (a) and (b). The dark portion represents target presence and is marked by data tip which indicate location as 1.35m in Fig.4 (a) and 1.8m in Fig.4 (b) for second data set and third set respectively.



(a) Second data set

(b) Third data set

Fig. 4. Range profiles in the presence of human target

From the Fig. 4 (a) and (b), it is clearly observed that for the first three peaks there is no amplitude variation. But for the fourth peak, amplitude variations are observed.

C. Raw Image

Raw image is *formed* by stacking all the range profiles [18]. The dimensions of raw image are obtained such number of traces are on x-axis and distance is represented on y-axis. Raw images as shown in Fig.5 (a) and (b) for second and third data set are obtained. It can be observed from Fig.5 (a) and (b) that the amplitudes of the clutter are higher than target reflection. Because of weak human target strength, the reflections are not visible. Reduction in clutter amplitude will improve strength of the human target signal which is described below.

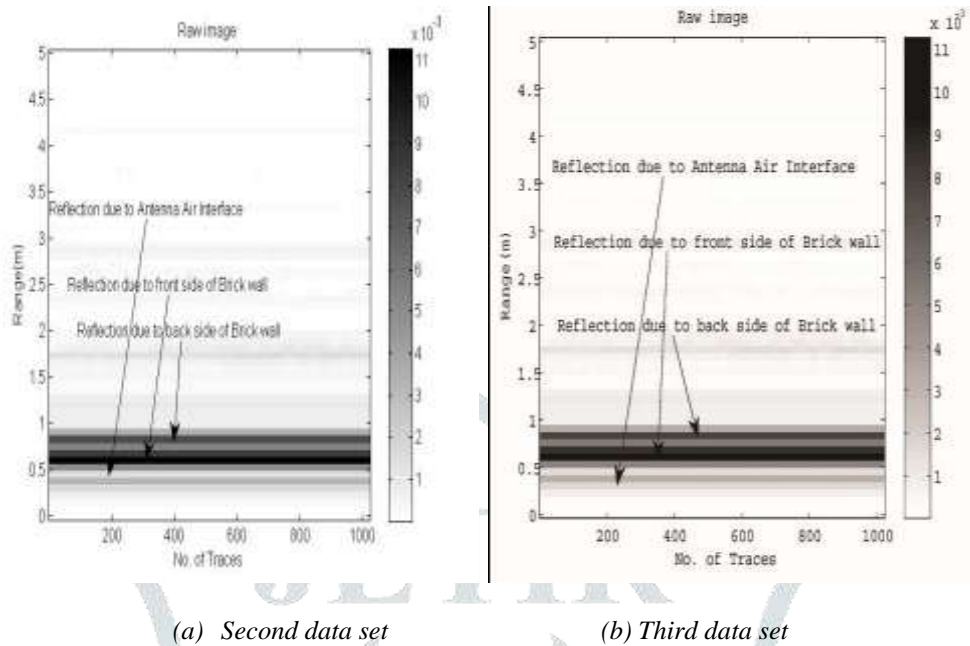


Fig.5. Raw image

D. Improvement in Detection

The technique to reduced clutter as described in step 5 of Fig. 2 is applied on raw image and results are obtained as shown in Fig.6 (a) and (b). From Fig.6 (a) and (b), the variation at target location can be easily observed due to life sign of human target. In Fig. 6 (a), data tip marked value as 1.35 m which is target location and as indicates variations in gray shades along x-axis. Similarly from Fig. 6 (b), data tip marked value as 1.8 m where amplitude variations are observed along x-axis. From these results, enhanced target signal strength with reduction in clutter is observed. Performance of clutter reduction technique is measured by calculating average target signal strength. For second data set, the average signal strength value at target position before and after clutter reduction are 0.045 and 0.2732. Clutter reduction is done using only second singular components using (9). The average signal strength value is further improved when seven singular components related to target subspace are used to form target image as described in (10) to 0.3777. These are obtained by observing range profiles for each singular components. If the target reflection is observed then that singular component is considered for forming target image. All such singular components are used to form final target image. The final image is formed after adding all images corresponding to seven Singular components i.e., second, third, fourth, fifth, sixth, seventh and eighth is shown in Fig. 7(a). For the third data set, the average signal strength is 0.0055 before clutter reduction and after clutter reduction using only second Singular component, it is improved to 0.3950. When the three Singular components i.e., second, third and fourth are used, the average signal strength is further increased to 0.4436. The final image formed after adding all images corresponding to three Singular components i.e., second, third and fourth, is shown in Fig. 7(b). It is observed from the results that, as the distance between radar and target is increased, the number of singular components related to target subspace are reduced. Thus enhanced signal strength at location of target is observed either using single singular component or multiple singular components related to target space are taken.

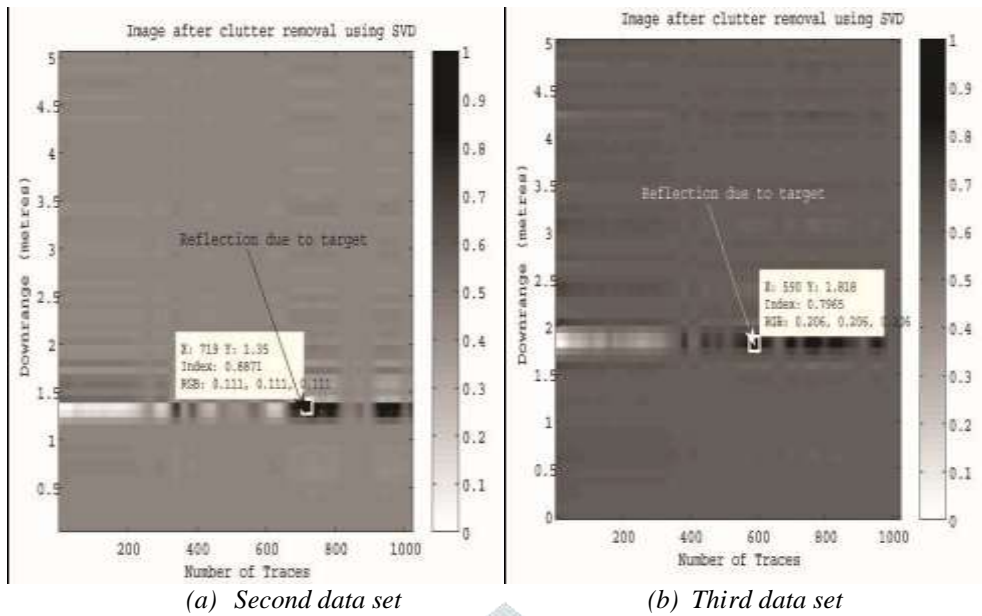


Fig.6. Image after clutter reduction

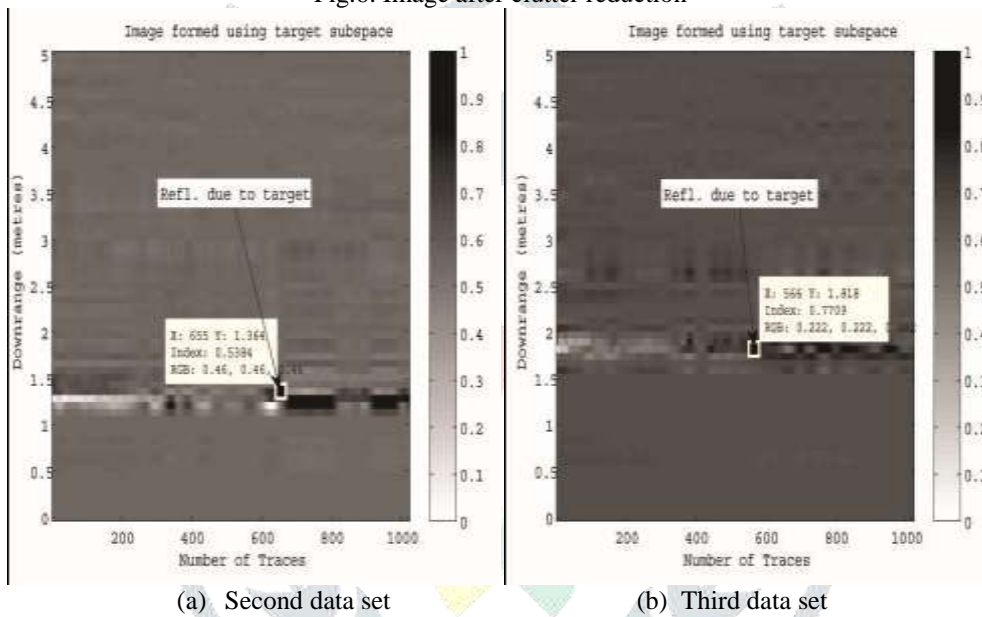


Fig.7. Image formed using Target Singular Components

E. Location Determination using SD

For location of human target, calculation of SD is carried out at all distance using (11). At human target location, value of SD is high compared to location of static objects in scene of measurements. The location is verified and is same as set during experimental setup. Table 3 gives SD values for both data sets. The location at which SD is highest is obtained by using index value. From Table 3, for the second data set, the index value obtained is 18 which gives distance as 1.35m. Index value is converted into distance by multiplying it by range resolution of 0.075. Similarly for third data set, the index value is 25 and the distance obtained is 1.8 m. If we compare the result obtained in Table 3 and result obtained in Fig. 4, the target locations in both cases are same. Thus it confirms that SD can be used to find location and presence of target.

Table 3. Location of target obtained using sd

Experiment Data	Maximum SD value	Index /location at which maximum SD occurs	Actual Location of target after correction (m)
Second Set of Experiment	0.0253/0.0270	18/1.35m	1.05
Third Set of Experiment	0.0112/0.0120	25/1.8m	1.5

Due to presence of brick-wall, the location of the target is different from actual. In the second data set, after processing the distance obtained is 1.35 m which is shown in Fig. 4 (a) with data tip. But during experimentations the distance was kept as 1m. Therefore velocity correction by using (12) is done to obtain actual location.

$$d_{true} = d_{observed} - d_{wall}(\sqrt{\epsilon_r} - 1) \quad (12)$$

where $d_{observed}$ is observed distance from Fig. 4 (a) which is 1.35m, d_{wall} is thickness of brick-wall which is 0.1 m and ϵ_r is average dielectric constant which is taken as 9 for the brick-wall. After using external metal calibration, which gives shift of 0.1m, the calculated location is 1.05m as shown in Table 3. The error for the second data set is 0.05m whereas for third data set, error is zero. Since the resolution of radar system is 0.075 m, the error of 0.05 m is in acceptable range.

F. FFT Results

After finding location of target, process described in step 6 of Fig. 2, is applied. It is observed that the adjacent position also has significant amplitude variations. So, three amplitude values are selected i.e., the location at which SD is maximum, its preceding and succeeding location. The average of three locations amplitude is taken as input to FFT. Assuming normal breathing frequency range as 0.2-0.5 Hz for human, a band pass filter is used. The result obtained after FFT is shown in Fig. 8 (a) for second data set and in Fig. 8(b) for third data set. The frequency components of interest are chosen by observing largest amplitude. The frequencies observed are 0.4102 Hz and 0.3125 Hz respectively. Similar results are obtained if image after clutter reduction using all target subspace is used. So the breaths/min would be at about 24 and 19 respectively. From Fig. 8, other smaller peaks are observed which are probably due to harmonics of breathing frequencies or clutter.

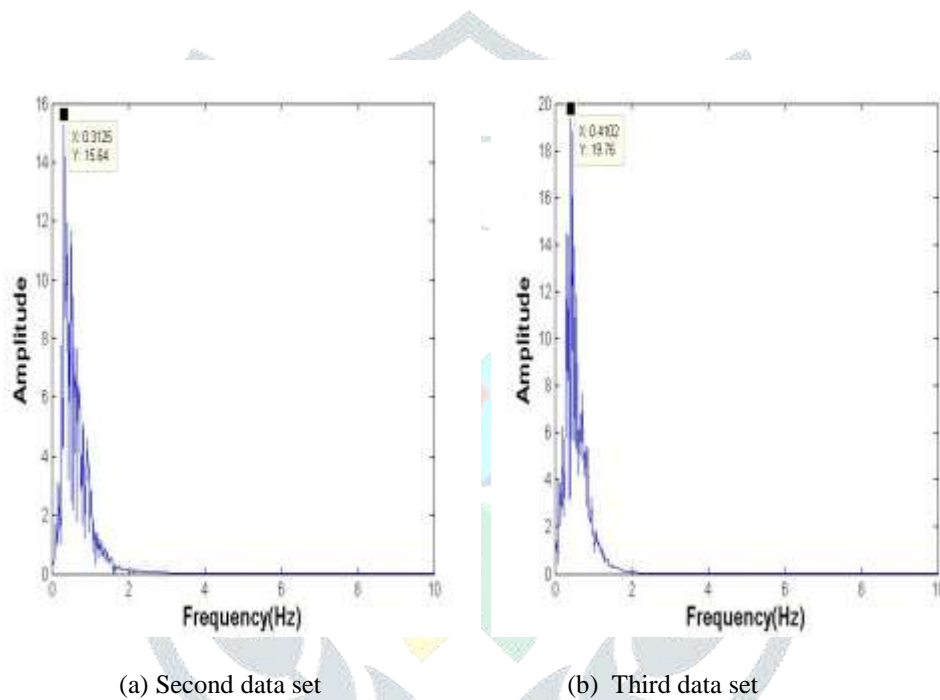


Fig.8. Frequency Spectrum

Concluding remarks

The objective of this paper is to improve the detection and extraction of breathing frequency of human being positioned behind the brick-wall using SFCW radar system in UWB frequency range. After applying clutter reduction technique using SVD, clutters are successfully minimized which implies that the technique is powerful. Target signal strength is improved further by using all singular components related to target. Due to the use of clutter reduction technique, the probability of correct detection of target increases. Increase in target signal strength is useful for process of extraction of life sign signal. Extraction of breathing frequency as well as determination of location is achieved in this paper. The determination of higher SD value helps in the automatic indication of presence of life sign signal of a human being along with location. The experimental results also show that FFT method is useful for extraction of breathing frequency of human being after using band pass filter. From the results obtained using second and third data set, it is observed that as the distance to human target increases, the amplitude of breathing signal reduces. Extraction of heart beat frequency can be carried out in future using advance signal processing techniques. In future study, brick-wall can be replaced by different complex type of brick-walls like concrete with metal inside and its effect on the detection can be studied.

ACKNOWLEDGMENT

Author would like to acknowledge UGC, New Delhi, for sanction of funds under major research project scheme (MRP F.No. 43-306/2014 (SR) dated 05 Sep. 2015. Author also thanks the students of final year project batch for their valuable assistance in data collection. Thanks are also extended to Head of Department, Electronics and Telecommunication, Dr. N P Jawarkar, Principal Dr. H B Nanvala of our Institute, Babasaheb Naik College of Engineering Pusad and the Management Janata Shikshan Prasarak Mandal, Pusad for encouraging and providing the necessary facilities.

REFERENCES

- [1] D.D. Ferris Jr. and N.C. Currie. 1998. A survey of current technologies for through-the-wall surveillance (TWS). Proceedings of SPIE, vol. 3375, pp. 62-72.
- [2] L. Liu and S. Liu. 2014. Remote Detection of Human Vital Sign With Stepped-frequency continuous wave radar. IEEE journal of selected topics applied earth observations and remote sensing, vol. 7, no. 3, pp. 775-782.
- [3] K. Chen, Y. Huang, J. Zhang, and A. Norman. 2000. Microwave life-detection systems for searching human subjects under earthquake rubble and behind barrier. IEEE Trans. Biomed Eng., vol. 27, no.1, pp.105-114.
- [4] D. D. Ferris Jr. and N. C. Currie. 1998. Microwave and millimeter wave systems for wall penetration. Proceedings of SPIE, vol. 3375, pp. 269-279.
- [5] R. M. Narayanan 2008. Through-wall radar imaging using UWB noise waveforms. J. Frankl. Inst., vol. 345, no. 6, pp. 659–678.
- [6] Y. Zhang *et al.* 2012. A detecting and identifying method for two stationary human targets using single-channel ultra-wideband radar. EURASIP J. Adv. Signal Process., vol. 202, pp. 1-6.
- [7] Y. Wang, Q. Liu, and A. Fathy. 2013. CW and Pulse, "Doppler Radar Processing Based on FPGA for Human Sensing Applications. IEEE Trans. Geosci. Remote Sens., vol.56, no. 5, pp. 3097–3107.
- [8] L. Liu, Z. Liu, and B. E. Barrowes. 2011. Through-Wall Bio-Radiolocation With UWB Impulse Radar: Observation, Simulation and Signal Extraction. IEEE J. Sel. Top. Appl. Earth Obs. Remote Sens., vol. 4, no. 4, pp. 791–798.
- [9] P.K. Verma, A.N. Gaikwad, D. Singh, and M.J. Nigam. 2009. Analysis of clutter reduction techniques for through wall imaging in UWB range. Progress in Electromagnetic Research B, vol. 17, pp. 29-48.
- [10] A.N. Gaikwad, D. Singh and M.J. Nigam. 2011. Application of clutter reduction techniques for detection of metallic and low dielectric target behind the brick wall by stepped frequency continuous wave radar in ultra-wideband range. IET Radar, Sonar and Navigation, vol. 5, pp. 416-425.
- [11] R. Chandra, A. N. Gaikwad, D. Singh and M. J. Nigam. 2008. An approach to remove the clutter and detect the target for ultra-wideband through-wall imaging. Journal of Geophysics and Engineering, vol. 5, pp. 412-419.
- [12] A. Nezirovic, A. G. Yarovoy and L. P. Ligthart. 2010. Signal Processing for Improved Detection of Trapped Victims Using UWB Radar. IEEE Trans. Geosci Remote Sens, vol. 48, no. 4, pp. 2005-2014.
- [13] M. G. Amin and F. Ahmad. 2013. Change Detection Analysis of Humans Moving Behind Walls. IEEE Trans. Aerosp. Electron. Syst., vol. 49, no. 3, pp. 1410-1425.
- [14] M. D'Urso, F. Gianota, R. Lalli, and L. Infante. 2010. Differential approach for through-the-wall life signs detection. Proc. IEEE Int. Radar Conf., pp. 1079–1082.
- [15] Z. Zhang, X. Zhang, H. Lv, et.al. 2013. Human-Target Detection and Surrounding Structure Estimation Under a Simulated Rubble via UWB Radar. IEEE Geosci. Remote Sens. Lett., vol. 10, no. 2, pp. 328–331.
- [16] Y. Xu, J. Shao, J. Chen, and G. Fang. 2013. Automatic Detection of Multiple Trapped Victims by Ultra-Wideband Radar. IEEE Geosci. Remote Sens. Lett., vol. 10, no. 6, pp. 1498–1502.
- [17] Y. Jia, L. Kong, X. Yang and K. Wang. 2013. Through-wall-radar Localization for Stationary Human Based on Life-sign Detection," IEEE Radar Conference, Ottawa, , pp. 1-4.
- [18] Y.S., Yoon, and M.G. Amin. 2009. Spatial filtering for wall-clutter mitigation in through the wall radar imaging. IEEE Trans. Geosci. Remote Sens., 47, pp.3192–3208.
- [19] Y.Xu, et.al. 2012. Vital Sign Detection Method Based on Multiple Higher Order Cumulant for Ultrawideband Radar. IEEE Trans. Geosci. Remote Sens., vol.50, no.4.pp.1254–1265.
- [20] F. H. C. Tivive, A. Bouzerdoum and M. G. Amin.2015. A Subspace Projection Approach for Wall Clutter Mitigation in Through-the-Wall Radar Imaging. IEEE Trans. Geosci. Remote Sens., vol. 53, no. 4, pp. 2108-2122.
- [21] M. Mabrouk, S. Rajan, M. Bolic, I. Batkin, H. R. Dajani and V. Z. Groza. 2014. Detection of human targets behind the wall based on singular value decomposition and skewness variations. IEEE Radar Conference, pp. 1466-1470.
- [22] T. C. Chen, J. H. Liu, P. Y. Chao and P. C. Li. 2015. Ultrawideband Synthetic Aperture Radar for Respiratory Motion Detection. IEEE Trans. Geosci. Remote Sens., vol. 53, no. 7, pp. 3749-3763.
- [23] L.Kong, T. Su, G. Cui, J. Yang. 2009. Life detection algorithm for stepped-frequency CW radar. IET Int. Conf., pp.271–350.
- [24] A. N. Gaikwad, U. S. Verulkar and K. S. Dongre. 2016. Experimental study and analysis of stepped-frequency continuous wave based radar for through the wall detection of life signs. IEEE Region 10 Conference (TENCON), Singapore, pp. 1565-1569.
- [25] A. Sume *et al.* 2011. Radar Detection of Moving Targets Behind Corners. IEEE Trans. Geosci. Remote Sens., vol. 49, no. 6, pp. 2259–2267.
- [26] S. Singh, Q. Liang, D. Chen, and L. Sheng. 2011. Sense through wall human detection using UWB radar. EURASIP J. Wirel. Commun. Netw., vol. 2011, no. 20, pp. 1-11.
- [27] M. Ascione, A. Buonanno, M. D'urso, L. Angrisani, and R. S. L. Moriello. 2011. Distributed sensing in homeland security applications," in IEEE International Workshop on Measurements and Networking Proceedings (M&N), Anacapri, pp. 16–21,.
- [28] M. Ascione, A. Buonanno, M. D'Urso, L. Angrisani, and R. Schiano Lo Moriello. 2013. A New Measurement Method Based on Music Algorithm for Through-the-Wall Detection of Life Signs. IEEE Trans. Instrum. Meas., vol. 62, no. 1, pp. 13–26.
- [29] Y. Xu, S. Dai, S. Wu, J. Chen, and G. Fang. 2012. Vital Sign Detection Method Based on Multiple Higher Order Cumulant for Ultrawideband Radar. IEEE Trans. Geosci. Remote Sens., vol. 50, no. 4, pp. 1254–1265.
- [30] Y.Xu, S.Wu, C.Chen, J. Chen and G. Fang. 2012. A Novel Method for Automatic Detection of Trapped Victims by Ultrawideband Radar. IEEE Trans. Geosci. Remote Sens., vol. 50, no.8, pp.3132-3142.
- [31] A. P. Freundorfer and K. Iizuka. 1993. A study on the scattering of radio waves from buried spherical targets using the step frequency radar. IEEE Trans. Geosci. Remote Sens., vol. 31, no. 6, pp. 1253-1255.